

# A kinematically distinct core and minor-axis rotation: the MUSE perspective on M 87

Eric Emsellem,<sup>1,2\*</sup> Davor Krajnović,<sup>3</sup> Marc Sarzi<sup>4</sup>

<sup>1</sup>European Southern Observatory, Karl-Schwarzschild-Str. 2, 85748 Garching, Germany

<sup>2</sup>Université Lyon 1, Observatoire de Lyon, Centre de Recherche Astrophysique de Lyon and Ecole Normale Supérieure de Lyon, 9 avenue Charles André, F-69230 Saint-Genis Laval, France

<sup>3</sup>Leibniz-Institute für Astrophysics Potsdam (AIP), An der Sternwarte 16, D-14482 Potsdam, Germany

<sup>4</sup>Centre for Astrophysics Research, University of Hertfordshire, Hatfield, Herts AL1 9AB, UK

1 October 2018

## ABSTRACT

We present evidence for the presence of a low-amplitude kinematically distinct component in the giant early-type galaxy M 87, via datasets obtained with the SAURON and MUSE integral-field spectroscopic units. The MUSE velocity field reveals a strong twist of  $\sim 140^\circ$  within the central  $30''$  connecting outwards such a kinematically distinct core to a prolate-like rotation around the large-scale photometric major-axis of the galaxy. The existence of these kinematic features within the apparently round central regions of M 87 implies a non-axisymmetric and complex shape for this galaxy, which could be further constrained using the presented kinematics. The associated orbital structure should be interpreted together with other tracers of the gravitational potential probed at larger scales (e.g., Globular Clusters, Ultra Compact Dwarfs, Planetary Nebulae): it would offer an insight in the assembly history of one of the brightest galaxies in the Virgo Cluster. These data also demonstrate the potential of the MUSE spectrograph to uncover low-amplitude spectral signatures.

**Key words:** galaxies: elliptical and lenticular, cD – galaxies: kinematics and dynamics – galaxies: structure – galaxies: nuclei

## 1 INTRODUCTION

M 87 is the second brightest galaxy of the Virgo cluster, after M 49, M 86 being the third most luminous member. Galaxies in the Virgo cluster mainly concentrate around these three giant early-type galaxies with the largest sub-structure centred on M 87 (Virgo A), the other two (Virgo B and C) respectively around M 49 and M 60. M 87 itself is an extreme system, often classified as a cD due to its diffuse stellar envelope and halo (Weil, Bland-Hawthorn & Malin 1997; Mihos et al. 2005), and with a mass in stars of about  $10^{12} M_\odot$  (e.g. ?Murphy, Gebhardt & Adams 2011; ?). M 87 lies close to the centre of mass of the Virgo cluster as traced by the X-ray emission (Böhringer et al. 1994; Churazov et al. 2008). It hosts an active supermassive black hole of a few billion solar masses (Sargent et al. 1978; Macchetto et al. 1997; Gebhardt et al. 2011; Walsh et al. 2013), responsible for the triggering of a well-known radio jet (Biretta, Stern & Harris 1991), and is surrounded by more than 10,000 globular clusters (GCs, Peng et al. 2008, and Durrell et al., submitted). Its relative proximity (with a mean distance of 16.5 Mpc for the Virgo cluster, and a distance of 16.7 Mpc for M 87, Mei et al. 2007) made it a target of choice for numerous studies.

Galaxy merging is assumed to play a prominent role in the

hierarchical formation and evolution of such massive galaxies in clusters. A picture including a two-phase formation scenario recently emerged, with a first early gas-rich and violent merging stage, and a second less dramatic assembly stage when stars are being accreted as stellar systems merge with the existing central object (see e.g. De Lucia & Blaizot 2007; Khochfar & Silk 2009; Oser et al. 2010). This history can in principle be traced in today’s stellar population mix as well as in the stellar kinematics of the galaxy. In that context, sub-structures such as kinematically decoupled cores (Franx & Illingworth 1988; Jędrzejewski & Schechter 1988; Bender 1988), or kinematically distinct components (KDC) as quantitatively defined in Krajnović et al. (2011), and triaxial figures have been called as important signatures of the violent merging past. For instance, major galaxy mergers are expected to produce specific orbital stellar structures, and leave an imprint on the observed velocity moments (Balcells & González 1998; Hernquist & Barnes 1991; Jesseit et al. 2007; Hoffman et al. 2010; Bois et al. 2011). KDCs have been observed in many early-type galaxies (Davies et al. 2001; Emsellem et al. 2004; Krajnović et al. 2011), and the modelling of the stellar kinematics led to interesting constraints on their intrinsic structures (Statler et al. 2004; van den Bosch et al. 2008).

Many past studies have reported observed stellar kinematics of M 87, via long-slit spectroscopy (e.g. Sargent et al. 1978;

\* E-mail: eric.emsellem@eso.org

Davies & Birkinshaw 1988; Jarvis & Peletier 1991; van der Marel 1994b; Bender, Saglia & Gerhard 1994) and integral-field units (IFUs, see e.g. Emsellem et al. 2004; Gebhardt et al. 2011; Murphy, Gebhardt & Adams 2011). Most of these studies emphasise the lack of mean stellar rotation in M87, consistent with the very low ellipticity within the central  $30''$ . The isophotes have an increasing flattening towards the outer parts reaching an ellipticity  $\epsilon \sim 0.4$  at radial distances of a few hundreds of arcseconds (Carter & Dixon 1978; Liu et al. 2005). Davies & Birkinshaw (1988) tentatively suggested a minor-axis rotation (around a PA of  $80^\circ$ ) at an amplitude of about  $20 \text{ km s}^{-1}$ , although this result was cautiously flagged as marginally significant considering the modest signal-to-noise ratio of the dataset. However, Jarvis & Peletier (1991) reported mean stellar rotation along the minor-axis emphasising that "M87 is not an oblate rotator". The stellar halo of M87 was also probed with the VIRUS-P IFU, and Murphy, Gebhardt & Adams (2011) seem to detect mild rotation at large radii although it is not clear from their Figure 4 alone along which axis. More recently, a clear rotation pattern with an amplitude of  $\sim 20 \text{ km s}^{-1}$  was revealed by the multi-slit approach of Arnold et al. (2013): the stellar rotation axis at a radius of  $80''$  is not too far from the photometric major-axis of the galaxy. M87 has been modelled either as a spherical galaxy (e.g. van der Marel 1994b,a; Zhu et al. 2014) or as an oblate system (e.g. Gebhardt & Thomas 2009)

The central region of M87 has been recently observed with the MUSE spectrograph mounted at the ESO Very Large Telescope (Paranal, Chile). In this letter, we thus revisit the stellar kinematics of M87 within the central  $30''$  ( $\sim 2.5 \text{ kpc}$ ) using integral-field spectroscopy, and reveal the presence of a KDC in the central region of M87 using both SAURON and MUSE. We also clearly detect the signature of a prolate-like (minor-axis) rotation at a radius of about  $30''$ . In Section 2, we present the datasets, and the associated data reduction and analyses we have performed. In Section 3, we focus on the resulting stellar kinematic maps and the revealed kinematic structures. We briefly discuss these results in Section 4 and conclude.

## 2 DATA REDUCTION AND ANALYSIS

We describe here the SAURON and MUSE datasets that we are using to derive the stellar kinematics. We focus on the extraction of the stellar kinematics and concentrate in particular on the stellar velocity maps. A more complete description of the MUSE observations for M87, the data reduction and data quality assessment will be presented elsewhere (Sarzi et al., in prep.).

### 2.1 SAURON Data

M87 has been observed with the SAURON spectrograph (Bacon et al. 2001), an IFU installed at the William Herschel Telescope in the Canary Islands. The dataset was obtained in the course of the SAURON project (de Zeeuw et al. 2002) during Run #5 (for details, see Emsellem et al. 2004), and corresponds to the merging of 3 SAURON fields. Final spaxels before adaptive binning is performed are squared with  $0''.8$  on the side, the spectral sampling and instrumental dispersion ( $\sigma_{\text{spec}}$ ) being 60 and  $98 \text{ km s}^{-1}$ , respectively. We re-analysed the SAURON M87 dataset proceeding in the same fashion as described in Emsellem et al. (2004) and Cappellari et al. (2011), but this time trying to probe low amplitude velocity structures within the central region (see

Krajnović et al. 2011; Emsellem et al. 2011). We therefore use a significantly higher threshold for the Voronoi binning scheme (Cappellari & Copin 2003) with a minimum signal-to-noise ratio (SNR) of 300. Note that this value is only set as a relative goal as systematics do not ensure that the actual SNR increases steadily as spaxels are accreted.

### 2.2 MUSE Data

M87 has recently been observed in the context of Programme 60.A-9312 (PI Sarzi) of the first MUSE Science Verification run conducted with the Very Large Telescope at Paranal. MUSE delivers an impressive set of 90,000 spectra covering most of the optical domain from about 4800 to 9000 Å with a spectral instrumental dispersion of about  $60 \text{ km s}^{-1}$  at 5500 Å, and a field of view of nearly  $1'$  square sampled in rectangular  $0''.2 \times 0''.2$  spaxels. The central regions of M87 were observed for 1h, and after reducing the data with version 0.18.1 of the MUSE pipeline (to be described in Weilbacher et al., in prep.) these data delivered a mean SNR of 24 per spaxel at 5100 Å (for details on the observations, data reduction and quality assessment, see Sarzi et al. in prep). For consistency with our re-analysis of the SAURON data, we then spatially binned this datacube to achieve a similar target SNR of 300 using the Voronoi binning scheme.

### 2.3 Stellar kinematics

To extract the stellar kinematics from both the SAURON and MUSE dataset we used the penalised pixel fitting algorithm (pPXF) developed by Cappellari & Emsellem (2004). For the SAURON data, we used the same mixed library of stellar and population model templates and the same pPXF setup as done in Cappellari et al. (2011) in the case of the entire ATLAS<sup>3D</sup> early-type galaxy sample (see also Emsellem et al. 2004). For the MUSE data, we applied pPXF to the 5050 – 6000 Å wavelength interval while excluding regions potentially affected by [N I] $\lambda\lambda 5198, 5200$  emission, adopting a 10<sup>th</sup> order additive polynomial correction for the continuum and using a set of pre-derived templates that are best suited to match the stellar populations of M87. The latter templates correspond to the best combination of stars in the entire MILES library (Sánchez-Blázquez et al. 2006; Falcón-Barroso et al. 2011) that match, with pPXF, nine high-SNR spectra obtained by co-adding all the MUSE spectra within the central  $3''$  and in eight  $3''$ -wide annular and circular apertures extending out to  $27''$  (see Sarzi et al. in prep). Fig. 1 illustrates the quality of the MUSE data and of our pPXF fit for three Voronoi binned spectra across the central  $1'$  of M87. We estimated the systematic uncertainty in the MUSE mean velocity measurements for these bins to be less than  $2 \text{ km s}^{-1}$  both from fitting the unresolved sky lines and from the high frequency noise locally derived from the map itself (Fig. 2).

## 3 THE CENTRAL VELOCITY FIELD OF M87

We first present the SAURON stellar velocity of M87 in the left panel of Fig. 2 where the Voronoi binning has been pushed up to reveal low amplitude structures. Two odd point-symmetric regions emerge. Firstly, the central  $15''$  exhibit a rotation-like pattern with an amplitude of about  $\pm 5 \text{ km s}^{-1}$  roughly aligned with the North-South direction, with the positive velocity in the North. Secondly, a rotation pattern ( $\pm 12 \text{ km s}^{-1}$ ) is visible at the edge of the SAURON field of view, but this time with an axis roughly perpendicular to

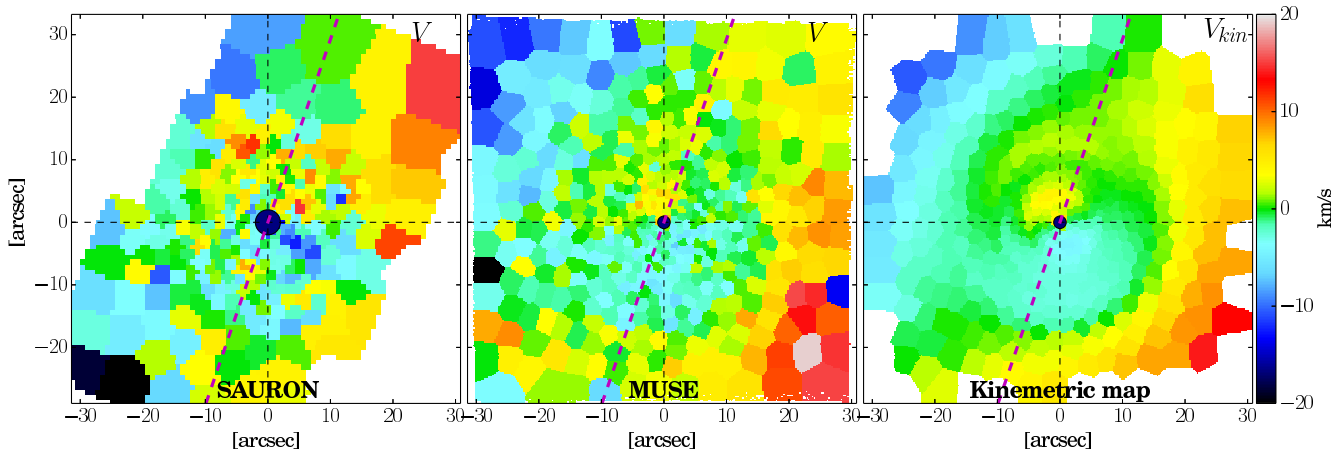


**Figure 2.** SAURON (left panel), MUSE (middle panel) and reconstructed kinematic (right panel) stellar velocity maps of the central region of M 87. The three red crosses in the middle panel correspond to the positions of the spectra shown in Fig. 1. The magenta dotted line marks the photometric major-axis of M 87 at large radii. North is up, and East is left. The central  $2''$  (left panel) or  $1''$  (middle and right panels), where the extracted kinematics is significantly affected by the presence of very broad and strong emission lines, are masked.

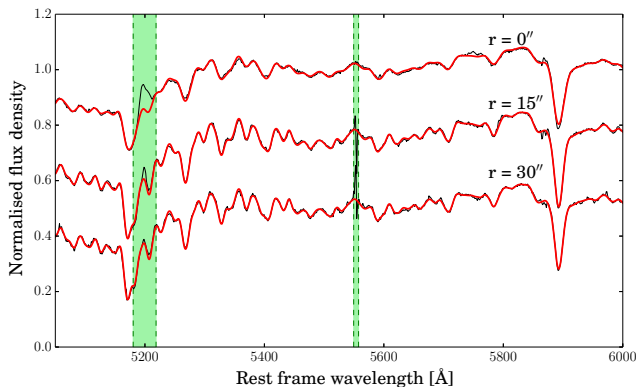


**Figure 1.** Three MUSE spectra (black lines) at three different radii (in the rest frame wavelength), with their corresponding pPXF fit (red lines). The two regions which were discarded from the fit are indicated by the filled green areas, the first corresponding to the  $[\text{N I}]\lambda\lambda 5198, 5200$  doublet, the second to a residual sky emission line.

the central rotation pattern. Even though the formal errors are relatively low, at a level of  $4 \text{ km s}^{-1}$  on average, the noise level is still high in this map due to the combined modest spectral resolution, systematics and the difficulty to extract accurate information from the SAURON short wavelength domain. This renders the detection of such low amplitude velocity structures tentative.

These features are, however, beautifully confirmed by the MUSE stellar velocity map (central panel of Fig. 2). The M 87 velocity field shows a kinematically distinct component within about  $15''$  twisting outwards connecting to a velocity pattern nearly symmetric around the photometric major-axis of the galaxy. To quantify this further, we applied the kinemetry (Krajnović et al. 2006) to the MUSE mean stellar velocity map, constraining the ellipticity of the fitted ellipse to be below 0.1, as to follow the underlying photometry. The resulting profiles for the position angle and velocity amplitude are presented in Fig. 3, and the velocity field reconstructed using only up to the first order kinematic harmonic is shown in Fig. 2 (right panel).

The resulting kinematic position angle (PA) exhibits a clear

and rather rapid change at a radius of  $\sim 15''$  where PA goes from a mean of  $17^\circ$  to about  $-124^\circ$  (or  $236^\circ$  when measured East of North). This kinematic twist of about  $140^\circ$  has the same sign, but a larger amplitude than the photometric twist (see e.g. Ferrarese et al. 2006), and is rather abrupt with a rapid transition region between  $15$  and  $20''$ . The misalignments of the inner and the outer components is significant, i.e., the components are not at  $180^\circ$  misalignment and, hence, not strictly counter-rotating. This suggests a triaxial structure with, under the assumption that the density of the galaxy is stratified on similar ellipses, a viewing angle likely not along, but not far from, the intrinsic long axis (Statler 1991). A more precise determination of the viewing angles requires the construction of detailed dynamical models (e.g. van den Bosch & van de Ven 2009), beyond the scope of this paper.

In the outer part, the axis of rotation is roughly aligned with the photometric minor-axis of M 87, hinting for a prolate-like rotation. The stellar kinematics observed at the edge of the MUSE field of view connect well with the structure observed at larger radii by Arnold et al. (2013). In Fig. 4, we also show that the MUSE stellar kinematics is indeed consistent with the (noisier) SAURON data, and with long-slit kinematics from Bender, Saglia & Gerhard (1994). The latter two include an odd symmetry in the radial velocity profile, but systematics are on the high side. This contrasts with the low systematics in the MUSE dataset which is reflected in the average velocity uncertainty of  $1.5 \text{ km s}^{-1}$ , with most of the formal errors ranging from  $1$  to  $2 \text{ km s}^{-1}$ . Note that the stellar velocity dispersion from SAURON and MUSE are consistent with each others, while the long-slit values from Bender, Saglia & Gerhard (1994) seem to overshoot in the outer part.

It is worth emphasising here that the present discovery of a central kinematically distinct component in the inner region of M 87 is an excellent illustration of the capabilities of an IFU like MUSE which should therefore become an instrument of choice when exquisite two-dimensional information with low systematics are needed.

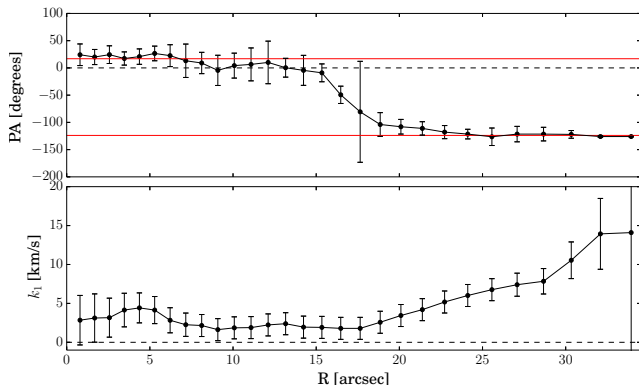


**Figure 3.** Position angle (top panel) and amplitude (bottom panel) from the extracted kinematic profiles of the MUSE stellar velocity field. The black dashed lines delineate the 0 and 360° limits, while the red dashed lines show the average PA values within 13'' and between 17 and 34'', respectively.

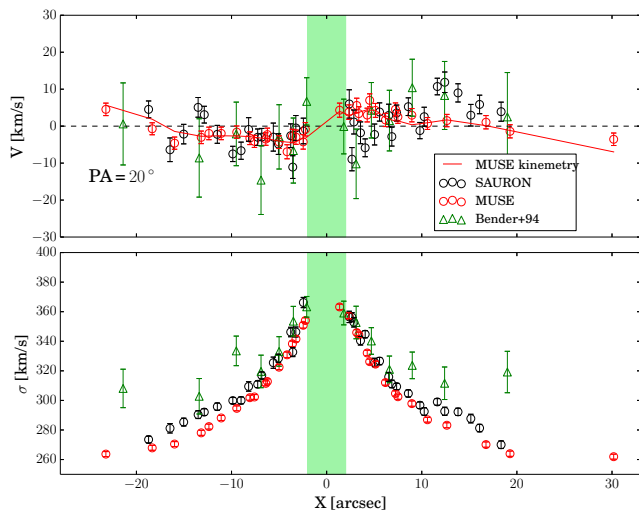


**Figure 4.** Cuts along a position angle  $PA=20^\circ$  of the MUSE (red circles) and SAURON (black circles) stellar velocity  $V$  (top panel) and velocity dispersion  $\sigma$  (bottom panel) fields. The long-slit kinematics along the same PA from Bender, Saglia & Gerhard (1994) are overlaid (green triangles). The red line shows the first harmonic kinematic fit to the MUSE velocity field. The green area shows the central 2'', where the SAURON kinematics is deemed not reliable.

#### 4 CONCLUDING REMARKS

We have shown evidence for the existence of a distinct kinematic component in the central 15'' of M87, using SAURON and MUSE integral-field data. The rotation pattern of the core is of low amplitude ( $\pm 5 \text{ km s}^{-1}$ ) and is offset by about  $30^\circ$  from the outer photometric major-axis. This connects via a  $140^\circ$  velocity twist to a minor-axis rotation in the outer part of the MUSE field. The classification of M87 as a “non-rotator” (Emsellem et al. 2004) should therefore be revised, with M87 joining the group of massive slow rotators with KDCs and outer minor-axis rotation such as NGC 4365 and NGC 4406 (Davies et al. 2001; Emsellem et al. 2004; Krajnović et al. 2011). This also questions the generic presence of KDCs in slow rotators (Emsellem et al. 2011; Krajnović et al. 2011), while already more than 60% of all slow rotators in the ATLAS<sup>3D</sup> sample have KDCs.

If the overall very low ellipticity of the isophotes in the cen-

tral  $30''$  is the result of a low inclination angle, this could imply a rather significant intrinsic mean stellar rotation in that region. However, it is worth noting that with a stellar velocity dispersion in excess of  $250 \text{ km s}^{-1}$  within  $30''$ , the central dynamics of M87 is very probably dominated by random motions. Still, the existence of the KDC and the measure of a velocity twist within its apparently round central region are key ingredients to constrain the viewing angles and the shape of M87. It first triggers a qualitative change of how we view the central region of this well-known massive galaxy: M87 is often considered as a spherical system while the present observations imply a complex non-axisymmetric structure with a radial change in the orbital configuration. As emphasised by van den Bosch & van de Ven (2009), the detection of a radial variation in the photometric position angle, and more importantly in the kinematic major-axis (hence with the zero velocity curve not being a straight line as in e.g., oblate systems, see Statler 1991) is also a crucial ingredient for the recovery of the intrinsic shape: it fundamentally helps shrinking the parameter space to probe with such modelling. This is particularly true for triaxial systems with KDCs where the uncertainty on the axis ratios is significantly reduced, even more so when a strong twist and misalignment are present (van den Bosch & van de Ven 2009).

As shown by Hunter & de Zeeuw (1992) for idealised models, the relative weights of the orbital families varies roughly like the square of the ratio between the long-axis and short-axis. From the observed KDC and kinematic twist, we can already assume a relative fractional increase of the importance of short-axis (resp. long-axis) tubes orbits in the inner (resp. outer) parts (see e.g. van den Bosch et al. 2008; Hoffman et al. 2010). A more quantitative assessment of the global dynamics and orbital structure of M87 would require detailed modelling of this new MUSE dataset, possibly complemented by a more extended MUSE mosaic, and adding e.g., the large-scale observations obtained by e.g., Arnold et al. (2013).

Numerical simulations also suggest that a global trend exists between the importance of in-situ versus ex-situ star formation and e.g., the mean stellar age for massive galaxies (Naab et al. 2014), and the orbital structure (Jesseit, Naab & Burkert 2005). The non-axisymmetry of M87 both in its central part as probed by the misaligned KDC and in the outer part with its minor-axis rotation already indicates a non-isotropic assembly. Minor mergers are thus often called upon for as an important ingredient for the assembly of massive galaxies in clusters (see e.g., Burke & Collins 2013). Naab et al. (2014) also emphasised the fact that the rare class of non-rotators has probably grown via the sole contribution of gas-poor minor mergers. The specific case of M87 may tell us otherwise, with major mergers being an interesting process to consider here, given that a single gas-rich major event may be able to account for a significant part of the observed complexity (Hoffman et al. 2010; Bois et al. 2011).

The present kinematic observations, associated with a detailed study of the stellar populations in these regions should provide further constraints on the merger history of M87. Other tracers such as Planetary Nebulae and Globular Clusters (Kissler-Patig & Gebhardt 1998; Côté et al. 2001; Peng et al. 2008; Doherty et al. 2009; Longobardi et al. 2013) or Ultra Compact Dwarfs (UCDs) could help nailing down its evolutionary path. An illustration of this comes from the recent claim by Zhang et al. (submitted) that the rotation axis of Ultra Compact Dwarfs (UCDs) orbiting M87 is roughly orthogonal to that of the blue GCs. This may be for M87 the potential missing link between the prolate-like rotation of its stellar component emphasised in the present paper and

the UCDs, while the blue GCs would follow a more natural rotation pattern around the outer photometric minor-axis of the galaxy. Whether UCDs are predominantly the remnants of harassed dwarfs, or the massive tail of stellar clusters formed during gas-rich merger events, a combined dynamical analysis of UCDs, GCs and stars in M 87 in comparison with hydrodynamical simulations would bring our understanding of these structures one step further. The ultimate goal would obviously be to reconcile all such signatures of the phase-space complexity of M 87 (Romanowsky et al. 2012; Murphy, Gebhardt & Cradit 2014) with a global view of its assembly history.

#### ACKNOWLEDGEMENTS

The authors would like to warmly thank the entire MUSE team, and its PI (Roland Bacon), for their many years of efforts to deliver such a remarkable instrument (hardware, operation software, advanced data reduction pipeline). We would like to thank the MUSE Science Verification support team, and Lodovico Coccato for comments on the data reduction. We also thank Tim de Zeeuw for valuable input and comments on an early version of this manuscript. EE dedicates this paper to Thilo.

#### REFERENCES

- Arnold J. A. et al., 2013, arXiv:1310.2607  
 Bacon R. et al., 2001, MNRAS, 326, 23  
 Balcells M., González A. C., 1998, ApJL, 505, L109  
 Bender R., 1988, A&A, 202, L5  
 Bender R., Saglia R. P., Gerhard O. E., 1994, MNRAS, 269, 785  
 Biretta J. A., Stern C. P., Harris D. E., 1991, AJ, 101, 1632  
 Böhringer H., Briel U. G., Schwarz R. A., Voges W., Hartner G., Trümper J., 1994, Nature, 368, 828  
 Bois M. et al., 2011, MNRAS, 416, 1654  
 Burke C., Collins C. A., 2013, MNRAS, 434, 2856  
 Cappellari M., Copin Y., 2003, MNRAS, 342, 345  
 Cappellari M., Emsellem E., 2004, MNRAS, 116, 138  
 Cappellari M. et al., 2011, MNRAS, 413, 813  
 Carter D., Dixon K. L., 1978, AJ, 83, 574  
 Churazov E., Forman W., Vikhlinin A., Tremaine S., Gerhard O., Jones C., 2008, MNRAS, 388, 1062  
 Côté P. et al., 2001, ApJ, 559, 828  
 Davies R. L., Birkinshaw M., 1988, ApJSS, 68, 409  
 Davies R. L. et al., 2001, ApJL, 548, L33  
 De Lucia G., Blaizot J., 2007, MNRAS, 375, 2  
 de Zeeuw P. T. et al., 2002, MNRAS, 329, 513  
 Doherty M. et al., 2009, A&A, 502, 771  
 Emsellem E. et al., 2011, MNRAS, 414, 888  
 Emsellem E. et al., 2004, MNRAS, 352, 721  
 Falcón-Barroso J., Sánchez-Blázquez P., Vazdekis A., Ricciardelli E., Cardiel N., Cenarro A. J., Gorgas J., Peletier R. F., 2011, A&A, 532, 95  
 Ferrarese L. et al., 2006, ApJSS, 164, 334  
 Franx M., Illingworth G. D., 1988, ApJL, 327, L55  
 Gebhardt K., Adams J., Richstone D., Lauer T. R., Faber S. M., Gültekin K., Murphy J., Tremaine S., 2011, ApJ, 729, 119  
 Gebhardt K., Thomas J., 2009, ApJ, 700, 1690  
 Hernquist L., Barnes J. E., 1991, Nature, 354, 210  
 Hoffman L., Cox T. J., Dutta S., Hernquist L., 2010, ApJ, 723, 818  
 Hunter C., de Zeeuw P. T., 1992, ApJ, 389, 79  
 Jarvis B. J., Peletier R. F., 1991, A&A, 247, 315  
 Jedrzejewski R., Schechter P. L., 1988, ApJL, 330, L87  
 Jesseit R., Naab T., Burkert A., 2005, MNRAS, 360, 1185  
 Jesseit R., Naab T., Peletier R. F., Burkert A., 2007, MNRAS, 376, 997  
 Khochfar S., Silk J., 2009, MNRAS, 397, 506  
 Kissler-Patig M., Gebhardt K., 1998, AJ, 116, 2237  
 Krajnović D., Cappellari M., de Zeeuw P. T., Copin Y., 2006, MNRAS, 366, 787  
 Krajnović D. et al., 2011, MNRAS, 414, 2923  
 Liu Y., Zhou X., Ma J., Wu H., Yang Y., Li J., Chen J., 2005, AJ, 129, 2628  
 Longobardi A., Arnaboldi M., Gerhard O., Coccato L., Okamura S., Freeman K. C., 2013, A&A, 558, 42  
 Macchetto F., Marconi A., Axon D. J., Capetti A., Sparks W., Crane P., 1997, ApJ, 489, 579  
 Mei S. et al., 2007, ApJ, 655, 144  
 Mihos J. C., Harding P., Feldmeier J., Morrison H., 2005, ApJL, 631, L41  
 Murphy J. D., Gebhardt K., Adams J. J., 2011, ApJ, 729, 129  
 Murphy J. D., Gebhardt K., Cradit M., 2014, ApJ, 785, 143  
 Naab T. et al., 2014, MNRAS, in press, 1311, 284  
 Oser L., Ostriker J. P., Naab T., Johansson P. H., Burkert A., 2010, ApJ, 725, 2312  
 Peng E. W. et al., 2008, ApJ, 681, 197  
 Romanowsky A. J., Strader J., Brodie J. P., Mihos J. C., Spitler L. R., Forbes D. A., Foster C., Arnold J. A., 2012, ApJ, 748, 29  
 Sánchez-Blázquez P. et al., 2006, MNRAS, 371, 703  
 Sargent W. L. W., Young P. J., Lynds C. R., Bokserberg A., Shortridge K., Hartwick F. D. A., 1978, ApJ, 221, 731  
 Statler T. S., 1991, AJ, 102, 882  
 Statler T. S., Emsellem E., Peletier R. F., Bacon R., 2004, MNRAS, 353, 1  
 van den Bosch R. C. E., van de Ven G., 2009, MNRAS, 398, 1117  
 van den Bosch R. C. E., van de Ven G., Verolme E. K., Cappellari M., de Zeeuw P. T., 2008, MNRAS, 385, 647  
 van der Marel R. P., 1994a, ApJL, 432, L91  
 van der Marel R. P., 1994b, MNRAS, 270, 271  
 Walsh J. L., Barth A. J., Ho L. C., Sarzi M., 2013, ApJ, 770, 86  
 Weil M. L., Bland-Hawthorn J., Malin D. F., 1997, AJ, 490, 664  
 Zhu L. et al., 2014, ArXiv e-prints, 1407, 2263